HHS Public Access

Author manuscript

Mol Genet Metab. Author manuscript; available in PMC 2022 August 01.

Published in final edited form as:

Mol Genet Metab. 2021 August ; 133(4): 362–371. doi:10.1016/j.ymgme.2021.06.001.

Pathogenic variants in *MRPL44* causes infantile cardiomyopathy due to a mitochondrial translation defect

Marisa W. Friederich[1,2], **Gabrielle C. Geddes**[3,4], **Saskia B. Wortmann**[5,6], **Ann Punnoose**[7], **Eric Wartchow**[2], **Kaz M. Knight**[1], **Holger Prokisch**[8,9], **Geralyn Creadon-Swindell**[2], **Johannes A. Mayr**[5], **Johan L.K. Van Hove**[1,2]

[1]Department of Pediatrics, Section of Clinical Genetics and Metabolism, University of Colorado, Aurora, CO, USA [2]Department of Pathology and Laboratory Services, Children's Hospital Colorado, Aurora, CO, USA [3]Department of Pediatrics, Medical College of Wisconsin, Milwaukee, WI, USA [4]Department of Molecular and Medical Genetics, Indiana University, Indianapolis, IN, USA [5]University Children's Hospital, Paracelsus Medical University (PMU), Salzburg, Austria [6]Amalia Children's Hospital, RadboudUMC, Nijmegen, The Netherlands [7]Herma Heart Institute, Children's Hospital of Wisconsin, Milwaukee, WI, USA [8]Institute of Neurogenomics, Helmholtz Zentrum München, Neuherberg, Germany [9]Institute of Human Genetics, Technical University of Munich, Munich, Germany

Abstract

Cardiac dysfunction is a common phenotypic manifestation of primary mitochondrial disease with multiple nuclear and mitochondrial DNA pathogenic variants as a cause, including disorders of mitochondrial translation. To date, five patients have been described with pathogenic variants in *MRPL44*, encoding the ml44 protein which is part of the large subunit of the mitochondrial ribosome (mitoribosome). Three presented as infants with hypertrophic cardiomyopathy, mild lactic acidosis, and easy fatigue and muscle weakness, whereas two presented in adolescence with myopathy and neurological symptoms.

We describe two infants who presented with cardiomyopathy from the neonatal period, failure to thrive, hypoglycemia and in one infant lactic acidosis. A decompensation of the cardiac function in the first year resulted in demise. Exome sequencing identified compound heterozygous variants in the *MRPL44* gene including the known pathogenic variant c.467T>G and two novel pathogenic variants. We document a combined respiratory chain enzyme deficiency with emphasis on complex I and IV, affecting heart muscle tissue more than skeletal muscle or fibroblasts. We show

Communicating author: Johan L.K. Van Hove, MD, PhD, MBA, Mailstop 8400, Education 2 South L28-4114, 13121 East 17th Avenue, Aurora, CO 80045, Tel. 303-724-2365, Fax 720-777-7322, Johan.Vanhove@childrenscolorado.org.

Competing interest statement:
JVH participates in clinical trials of mitochondrial disorders by Stealth Biotherapeutic, Inc. All other authors deny any real or apparent conflict of interest in the field of mitochondrial diseases.

Ethics: Studies were performed under the Institutional Review Board approved study COMIRB# 16-0146. Studies were performed under an ethics protocol of the Technical University München, 5360/12S.

this to be caused by reduced mitochondrial DNA encoded protein synthesis affecting all subunits, and resulting in dysfunction of complex I and IV assembly. The degree of oxidative phosphorylation dysfunction correlated with the impairment of mitochondrial protein synthesis due to different pathogenic variants. These functional studies allow for improved understanding of the pathogenesis of MRPL44-associated mitochondrial disorder.

Keywords

cardiomyopathy; combined deficiency; genetic cause; mitochondrial ribosome; mitochondrial translation

1. Introduction

Disorders of mitochondrial cellular energetics present with a wide spectrum of clinical symptoms. Cardiac involvement occurs in approximately half of all patients with mitochondrial diseases presenting in childhood [1]. Presentations can include congestive heart failure, dilated cardiomyopathy, hypertrophic cardiomyopathy, left ventricular non-compaction and cardiac fibrosis [2]. Cardiac involvement carries a worse prognosis than neuromuscular involvement [1]. The genetic cause for mitochondrial cardiomyopathies is highly heterogeneous and includes various pathogenic variants in mitochondrial DNA (mtDNA), as well as nuclear DNA causing isolated complex deficiencies, deficiencies of assembly factors, combined deficiencies of mitochondrial biogenesis, and disorders of the mitochondrial environment. Mitochondrial DNA encodes for 13 subunits of the respiratory chain complexes. These coding regions require transcription and translation process inside the mitochondria. Many disorders of the mitochondrial protein translation process are identified and include disorders of mitochondrial tRNAs or rRNAs, or nuclear encoded genes responsible for tRNA aminoacylation, or modification including formylation of the initiation methionine tRNA, proteins of the mitochondrial ribosome and ribosomal assembly proteins, and proteins involved in translation initiation, elongation, termination and release factors and translational activators [3]. Of these, cardiomyopathy has for instance been described in the following genes: *AARS2*, *YARS2*, *GARS*, *KARS*, *MRPL3*, *MRPS22*, *MRPS14*, *MRPL44*, *TSFM*, *RMND1, MTO1, HSD17B10, ELAC2, TRMT5, GTPBP3* [3].

Five patients have been described with compound heterozygous or homozygous pathogenic variants in *MRPL44* [4,5]. All patients presented as children with hypertrophic cardiomyopathy, had mild lactic acidosis, and easy fatigue and muscle weakness. The first child died in infancy of cardiac failure following an acute infection, whereas in her sister the cardiomyopathy stabilized, and she remained well with only asymptomatic cardiomyopathy at the time of publication at age 14 years [4]. Another child presented with cardiomyopathy, mild liver disease, and mitochondrial myopathy, but remained well at the time of publication at age 8 years [5]. Both these children have normal cognitive function [4,5]. The fourth patient from age 14 years on developed cardiomyopathy, hemiplegic migraines, learning difficulties, myopathy, tapetoretinal dystrophy, and Leigh-like lesions in thalami, basal ganglia and cerebellum on brain MRI [5]. A fifth patient presented as a young adult with skeletal myopathy and exercise intolerance, subclinical cardiac hypertrophy recognized at

age 21 years, migraine, transient episodes of neurological dysfunction of hemiparesis and confusion, spasticity and ataxia, and on brain MRI lesions in basal ganglia, thalami and midbrain and subcortical and cerebellar white matter [6]. She had normal cognitive function, but as a young adult started to have reduced processing speed and executive function. Patients who had heart and skeletal muscle biopsy examined showed a combined deficiency of complex I and IV [4,6], but only of complex IV in fibroblasts [4,5]. The variant c.467T>G; p.(Leu156Arg) is a commonly recurring causal pathogenic variant present in 9 of 10 alleles published (Supplemental Table 1), and was associated with reduced protein stability [4–6].

The protein product of the *MRPL44* gene, ml44, was identified as a component of the large subunit of the mitochondrial ribosome (mitoribosome) [7,8]. Mitochondrial ribosomes contain a small (28S) and a large subunit (39S). The large ribosomal subunit consists of the mtDNA encoded 16S rRNA and 52 nuclear-encoded mitochondrial ribosomal proteins (MRP) including mt-tRNA^{Val} as a structural subunit, whereas the small subunit has the mtDNA encoded 12S rRNA and 30 nuclear-encoded MRPs [9,10]. In the large subunit, only 28 proteins have homologues in bacteria, the other subunits including ml44 are unique to eukaryotes and their functions remain unclear [4]. In the expansion of the bacterial ribosome to eukaryotic mitochondrial ribosome, the ml44 protein was added early and is located near the peptide exit channel [10]. In yeast, it is present in the first assembly intermediate of the large mitoribosome [11]. In mice, it is expressed widely throughout multiple tissues during development and its absence is embryonically lethal [12].

It has an RNA binding domain (residues 236–306) and an RNase III-like domain (residues 86–228) although the latter is lacking critical residues and is likely non-functional [4]. It is uniquely located in the mitochondria where it forms a dimer and is associated with the large mitoribosome subunit [8]. It has a double band on the immunoblot of cardiac tissue [4]. The variant p.Leu156Arg, which is present in four patients [4–6], results in strongly reduced protein levels [4,6]. Downregulation of *MRPL44* transcription by siRNA resulted in decreased COX1 levels but not a decrease in mitochondrial protein translation products [4]. It resulted in a reduction in the amount of the assembled large mitoribosomal subunit, but not the small mitoribosomal subunit proteins [4]. In another downregulation experiment of stably transfected shRNA in NIH3T3 cells [9], mtDNA levels were maintained, but mtDNA-encoded RNAs were decreased and unprocessed tRNAs were increased, and protein translation was generally reduced with reduced levels of mtDNA-encoded proteins and resulting decreased oxidative phosphorylation (OXPHOS) capacity [9]. Proteins and 16S rRNA were decreased indicative of instability of the large mitoribosome [9]. A new putative role in the regulation or maturation of mtDNA-encoded RNA products has been proposed [9]. The reason for the differences in these results is unclear. In a patient homozygous for the common pathogenic variant, reduction in the large mitoribosome and reduced mitochondrial protein synthesis was noted [6].

We describe here two additional cases of children with compound heterozygous variants in *MRPL44*. Functional studies further describe the impact on mitochondrial function.

2. Case Reports

2.1 Case 1

This was the second child of non-consanguineous parents. During the pregnancy, there was concern that the fetus was small for gestational age and had an echogenic bowel, but this resolved prior to delivery. A prenatal TORCH infection evaluation was negative. Following vaginal delivery at $39^{6/7}$ weeks gestation, during the neonatal period the girl had an episode of hypothermia and was persistently hypoglycemic (lowest 16 mg/dL), which was treated with continuous intravenous glucose. A septic workup and evaluation for hyperinsulinism were unremarkable. She had feeding difficulties taking only 10 to 30% of her feeds orally with the remainder provided by nasogastric tube feeding. At 51 days of age, a chest radiograph identified cardiomegaly and an echocardiogram revealed an ejection fraction of 25% (normal 55–70%) with left ventricular dysfunction and hypertrophy. The patient responded well to treatment and was discharged at 71 days of life while being treated with beta blockers and receiving feeding mainly via gastrostomy tube. At this time, urine organic acids analysis showed elevated Krebs' cycle intermediates, an acylcarnitine profile showed elevated C2- and C5-dicarboxylylacylcarnitines but was otherwise unremarkable. Chromosomal microarray revealed a deletion of 16q23.3 (arr[hg19] 16q23.3 (83838395-84068625)X1), and a comprehensive cardiomyopathy sequencing panel did not report any variants.

Over the next months, the child showed adequate weight gain using gastrostomy feedings but remained unable to take adequate oral feedings. Her echocardiogram showed at four months an improved ejection fraction of 41%, which remained stable at eight months of age at 40%. Due to persistent concern for mitochondrial disease based on her multisystem involvement, poor growth, cardiac phenotype and history of hypoglycemia, the patient at this time underwent cardiac catheterization with myocardial biopsy and skeletal muscle biopsy for functional mitochondrial testing, followed by sequencing tests of whole exome and mitochondrial DNA. At nine months of age during a respiratory syncytial viral infection, she was admitted for hypoxia and had respiratory failure for ten days after which she recovered back to baseline. However, three days after discharge at ten months of age, she was readmitted in cardiogenic shock, hypotensive, hypoglycemic, lethargic and hypoxic, likely due to right ventricular failure. She required multiple inotropic medication, and placement of a Berlin heart left ventricular assist device, but still developed liver and renal dysfunction. She received venous to arterial extracorporeal membrane oxygenation (ECMO) support, followed by placement of a Berlin heart right ventricular assist device. She remained in cardiogenic shock and hepatic failure, and ultimately developed disseminated *Candida lusitanease* infection which resulted in her death two days after her first birthday.

Clinical exome sequencing demonstrated compound heterozygosity for pathogenic variants in the *MRPL44* gene (NM_022915.3): maternal c.481_484delinsTC; p.(Thr161Serfs*2), and paternal c.467T>G; p.(Leu156Arg), a previously reported missense pathogenic variant [4–6].

2.2 Case 2

This female was born as the first child of healthy non-consanguineous Caucasian parents at 39 weeks of gestation with normal Apgar scores of 9 at 1 min and 10 at 5 min, weight 3.560 kg, length 49 cm and head circumference 34 cm. She presented on the second day of life with Kussmaul breathing due to metabolic acidosis (pH < 7.0, base excess – 27 mEq/L), with elevated lactate 19 mmol/L (normal < 2 mmol/L) and mildly elevated ammonia 180 μM (normal < 100 μM). The physical examination was unremarkable. During the 5 weeks admission, she remained clinically stable with intermittently elevated lactate levels, and age-adequate development. She did not show signs of neurologic dysfunction, and had a normal brain ultrasound. Echocardiography at age days 15 and 29 showed a prominent left ventricle with normal function. She did have recurrent asymptomatic hypoglycemia (lowest glucose 40 mg/dL), with appropriate insulin, cortisol, and growth hormone response during hypoglycemia. The persistent lactic acidemia (3.3 to 15 mmol/L, normal < 2 mM) did not change in relation to feeding, the lactate/pyruvate ratio (lactate 9.5 mol/L, pyruvate 0.18 mmol/L, ratio 53 (normal <20) was elevated. Routine laboratory values of blood counts, transaminases, renal function, prothrombin time, and ammonia remained within normal limits. Plasma amino acids and acylcarnitines in dried blood spot were unremarkable, urinary organic acids were not performed.

A skin biopsy for fibroblast culture was obtained at age 5 weeks, and a skeletal muscle biopsy was performed at age 3 months. Histology showed some fibers with central cores and some hypercontracted fibers. Gomori trichrome staining did not reveal ragged blue fibers, and there were no cytochrome c oxidase negative fibers.

At age 6 months, she was admitted with worsening general condition. She had cardiomegaly on chest X-ray, and echocardiography showed a very restrictive right ventricle and a ballooned left ventricle with barely any unmeasurable contraction and blood flow, and she died in cardiac failure shortly after.

Exome sequencing done according to published protocols [13,14] showed compound heterozygosity for two variants in *MRPL44* (NM_022915.3) c.467T>C; p.(Leu156Pro), and c.467T>G; p.(Leu156Arg).

3. Methods

Studies were performed under the Institutional Review Board approved study COMIRB# 16-0146, and under an Ethics board approved protocol of the Technical University München, 5360/12 S.

3.1 Genetic testing

The presence of the variants was confirmed by Sanger sequencing. After DNA extraction from fibroblasts, PCR was performed followed by dideoxy-sequencing with primers as detailed in Supplemental Materials.

3.2 Cardiac histology

For electron microscopy examination, a portion of the heart biopsy was obtained and immediately fixed in cacodylate-buffered 2.5% glutaraldehyde before processing according to standard electron microscopy techniques, including secondary fixation in 2.0% osmium tetroxide, dehydration, and then embedding in epoxy resin. 80 nm ultrathin sections were poststained with uranyl acetate and lead citrate and imaged using a JEOL JSM-1400+ TEM (JEOL, Tokyo, Japan) equipped with a Gatan Orius SC1000B digital camera system (Gatan, Pleasanton, CA).

3.3 Mitochondrial functional studies

For Patient 1, respiratory chain enzyme activities were determined spectrophotometrically in a post 600 × g supernatant as described for muscle, heart, and fibroblasts [15,16]. Activities were expressed per mg protein, and as the ratio over the activity of citrate synthase and of complex II. The log transformed values of these activities and ratios in control samples were normally distributed, and patient activities can be expressed as Z-scores of this distribution. Further, respiratory chain complex activities were also analyzed by separation on a blue native gel and identification by in-gel activity staining as described before [15–17]. For Patient 2, respiratory chain enzyme activities were measured spectrophotometrically in fresh unfrozen muscle biopsy as described [18,19] and in fibroblasts as described [15,16]. Substrate oxidation rates in fresh muscle tissue was performed using various ^{14}C-labeled substrates as described [20].

The assembly of complex I was evaluated in mitochondrial membrane fractions isolated by differential centrifugation, solubilized, separated on a blue native gel, and after blotting probed with an antibody against NDUFS2 for the assembly of complex I and with an antibody against COX4 for the assembly of complex IV, subunits that are incorporated early as described [21]. The source and specifications of all antibodies used are listed in Supplemental Table 2.

3.4 Protein amount

The amount and the size of the ml44 protein in mitochondrial fractions isolated by differential centrifugation in skeletal muscle, heart and fibroblasts derived from Patient 1 and fibroblasts derived from Patient 2 and controls were evaluated by SDS-PAGE followed by western blot and detected using an antibody against ml44 protein. Furthermore, western blot analysis was performed on the 600 × g supernatants obtained from both control and Patient 1 skeletal muscle, heart tissue, and fibroblast and from Patient 2 fibroblasts using antibodies for both MT-CO1 and ATP5F1B. The synthesis of these proteins is more sensitive to mitochondrial translational defects.

3.5 Mitochondrial translation

The translation of mitochondrial proteins was evaluated in fibroblasts grown to 70–90%-confluency as described [22,23]. Fibroblasts were labeled by growing for 60 minutes in methionine and cysteine-free DMEM containing 200 μCi/ml of ^{35}S-methionine and ^{35}S-L-cysteine (EasyTag™ EXPRESS^{35}S Protein Labeling Mix, Perkin-Elmer) and 100 μg/ml of the cytoplasmic protein synthesis inhibitor emetine. Cells were harvested, resuspended in

200 μL phosphate buffered solution (PBS) and protein concentration was determined using the Bio-Rad protein assay. Between 30 to 50 μg cellular protein were then separated on a 15 to 20% gradient polyacrylamide denaturing gel. The gel was dried and the film developed by direct autoradiography to visualize the labeled mitochondrial translation products. A quantitative assay of mtDNA encoded protein synthesis was developed by harvesting the translation assay-labeled cells, and then resuspending the cells in 100–200 μL PBS as above. Four volumes of icecold acetone were added, samples were incubated at −20°C for at least 1 hour to precipitate proteins, and then pelleted by centrifugation for 10 min at 13,500 × g. After resuspending in 100 μL CelLytic™ M lysis buffer (Sigma), aliquots were analyzed by scintillation counting and protein concentration was determined using the Bio-Rad protein assay. The results were expressed as cpm/μg protein, which using the specific activity of the labeled amino acids allowed expression as fmol amino acid incorporated/ μg protein. Results were obtained from the average of six independent translation assays in Patient 1 fibroblasts and two independent translation assays in Patient 2 done in duplicate, and normal values were obtained from 17 control cell lines done in duplicate.

3.6 Respirometry

Cellular respiration was measured using an Oroboros Oxygraph 2k system following a substrate inhibitor (SUIT) protocol as described previously (17). Patient fibroblasts were assayed six times and compared to the data obtained from 41 control fibroblast cell lines, with the difference evaluated by Student t-test.

4. Results

In Patient 1, on electron microscopy, the heart showed areas of contractile element loss within the cardiomyocytes and a diffuse proliferation of enlarged, atypically shaped mitochondria with aberrant cristae, typical for a mitochondrial cardiomyopathy (Figure 1A,B). In Patient 2, on light microscopy skeletal muscle showed abnormal mitochondria with granular content and abnormal cristae, and in some fibers enlarged mitochondria were noted.

Sanger sequencing confirmed the presence of the variants identified on exome sequencing in the mitochondrial gene *MRPL44* (Supplemental Figure 1). The variant in Patient 1 c.481_484delinsTC p.Thr161Serfs*2 is predicted to cause either nonsense-mediated mRNA decay or a premature stop codon. The pathogenicity of the variant c.467T>G; p.Leu156Arg present in both patients was previously reported and causes protein instability [4,5]. The additional variant in Patient 2 affected the same amino acid Leu156, but the change was to proline instead of arginine. Substitutions to proline are generally strongly disruptive of secondary structure [24]. We thus expect that all variants decrease the amount of ml44 protein and we indeed found the amount of ml44 protein sharply reduced in all tissues examined for both patients (Figure 2A–D). Notable is the presence in patients' tissues of an additional band of slightly higher MW, which had already been noted in a patient homozygous for p.Leu156Arg. In fibroblasts only the band of increased MW is present (Figure 2C,D), whereas in heart muscle and skeletal muscle, both the band of normal MW and of increased MW is present (Figure 2A,B).

Pathogenic variants of mitoribosomal proteins are most likely to cause a deficiency of mitochondrial protein translation and thus a combined deficiency. Indeed, in Patient 1 respiratory chain enzyme activities showed a combined deficiency of the activities of respiratory chain enzyme complexes in heart tissue, with a profound decrease in complex IV and a strong decrease in complex I, and a mild decrease of complex II-III (Table 1). In skeletal muscle, there was increased activity in complex II and citrate synthase and relative to this a mild decrease in the activities of complexes I and IV. In fibroblasts, there was a borderline decreased activity of complex IV. On blue native PAGE with in-gel activity staining there is decreased staining of complex IV in heart, and in all three tissues heart muscle, skeletal muscle, and fibroblasts, there are bands of incompletely assembled complex V, more so in heart than in the other tissues (Figure 3A–C). In combination, these two functional studies indicate a combined deficiency affecting the complexes I, IV, and V, which have mtDNA encoded subunits. Further, the assembly of complex I shows multiple bands of incompletely assembled complex I in heart, muscle and fibroblasts (Figure 4A,C,D). Complex IV showed lesser amount of holocomplex at approximately 200 kDa (Figure 4E). The amount of MT-CO1 was decreased in all tissues, but the amount of ATP5FB1 was normal (Figure 2A–C). These results are consistent with a disorder affecting the synthesis of the proteins encoded by mtDNA.

In Patient 2, the respiratory chain enzyme activities in skeletal muscle showed a severe deficiency of complex IV activity and further deficiencies of the activities of complexes I, III, and V (Table 1). In fibroblasts the respiratory chain enzyme activities were normal in the 600 × g homogenate, but showed low complex IV activity in a mitochondrial isolate. The blue native PAGE with in-gel activity staining showed normal activities and normal complex V assembly (Figure 3D). Likewise, the complex I assembly assay did not show abnormal intermediates (Figure 4B), and the complex IV holoenzyme was normal (Figure 4F). However, similar to Patient 1, the amount of MT-CO1 was reduced compared to controls and the amount of ATP5FB1 was normal (Figure 2D).

A decrease in ml44 would affect the translation process on the mitoribosomes. We developed a quantitative assay of the synthesis of mtDNA encoded proteins by measuring the incorporation of ^{35}S-labeled sulfur amino acids into mitochondrial protein synthesis. The average incorporation of ^{35}S-labeled amino acids in control fibroblasts was 6.79 ± 3.22 fmol AA/μg protein (range 2.01–13.68 fmol AA/μg protein, n=17) whereas inhibition by the known mitochondrial protein synthesis inhibitor chloramphenicol showed an incorporation of ^{35}S-labeled sulfur amino acids of 2.27 fmol AA/μg protein. The fibroblasts of Patient 1 indeed had clearly decreased synthesis of mitochondrial proteins at 2.23 ± 0.48 fmol AA/μg protein, 33% of the average incorporation ($p<0.01$) (Figure 5A). The fibroblasts of Patient 2 had 3.8 ± 0.99 fmol AA/μg protein, 56% of average controls ($p=0.08$) (Figure 5A).

The activity of complex IV appeared more affected than that of other complexes in our patients. To evaluate if this was due to a differential effect on the rate of the synthesis of individual mtDNA-encoded subunits, we separated the labeled newly synthesized mitochondrial protein subunits on a gel and compared Patient 1 labeled products to in assay controls (Figure 5B). We found that the decrease in synthesis of complex IV encoded subunits COI 34.6±8.0%; COIII 29.8±8.9%; COII at 29.3% of concurrent control

fibroblasts, was similar to that of complex I encoded subunits: ND3 33.8±24%, ND2 32.2±7.2%, ND1 45.7%, ND5 63.9%, and ND6 21.2% of concurrent controls, and for complex V subunit ATP6 40.9±10.0% of concurrent control, and for complex III CYTB 60.15%. The average of all complex IV subunits was 30.1% whereas the average of all complex I subunits was 34.3%; these similar rates are not significantly different.

Functional impact of the mitochondrial dysfunction is shown on high resolution respirometry in fibroblasts of Patient 1 (Table 2). This showed low rates of oxygen consumption with all substrates, and a clear restriction of maximal rate after uncoupling, with limitation of the increase upon uncoupling resulting in increased coupling control ratio. Both the complex I and complex IV related rates are deficient, consistent with a combined deficiency. In muscle of Patient 2, there was low oxidation rates using both pyruvate and acetylcarnitine as substrates, although this was less evident after correction for citrate synthase (Supplemental Table 3). Thus, both patients showed metabolic dysfunction either as substrate or oxygen utilization as a result of the respiratory chain dysfunction.

5. Discussion

We present two patients with MRPL44-related mitochondrial disease. Clinically, both patients presented with a phenotype similar to previously reported patients with progressive and severe cardiomyopathy which became fatal in infancy, as well as recurrent hypoglycemia and failure to thrive, and in one patient lactic acidosis. As three of the previously five reported patients with cardiomyopathy did not develop systemic symptoms including neurodevelopmental involvement until the age of 8, 12, and 14 years, respectively, aggressive management including left ventricle assist device was performed in the case presented here. We were considering cardiac transplantation as an option in this condition in infancy, bearing in mind that in adolescence a progressive clinical involvement including neurological symptoms may still occur. An case of spontaneous resolution of cardiomyopathy after the first year was recently noted [30].

Genotypically, both patients had the known pathogenic variant c.467T>G; p.(Leu156Arg) in combination with a novel variant [4–6]. This variant is purported to leave some residual protein and activity. It is noteworthy that both patients presenting after infancy were homozygous for the c.467T>G; p.(Leu156Arg) pathogenic variant [4,6] (Supplemental Table 1). The variant c.481_484delinsTC; p.Thr161Serfs*2 causes a frameshift with premature stop codon, which would be expected to result in absent protein for this allele in Patient 1. In Patient 2, the variant c.467T>C; p.(Leu156Pro) affects the same amino acid Leu156 but a change to proline is considered particularly deleterious to the secondary structure of a protein usually resulting in strongly decreased, but not necessarily absent protein levels. Experimentally, in both patients the amount of ml44 protein was decreased. In addition to the decrease in abundance of the ml44 protein, it also appeared to have a slightly larger molecular weight. This may represent the retention of the mitochondrial leader peptide, which could be seen if the protein was not imported into the mitochondrion. Although this could not be quantified, from the genotype we would presume that Patient 1 (with a frameshift allele that results in absent protein) may be somewhat more affected

enzymatically than Patient 2 (with a missense allele that results in strongly reduced but not absent protein).

The ml44 protein is a subunit of the large mitoribosome. Reduced mitochondrial protein synthesis in a patient homozygous for c.467T>G was previously reported [6]. Indeed, protein synthesis of mtDNA-encoded subunits was decreased in fibroblasts from both patients, but the decrease was more pronounced in Patient 1 than in Patient 2. We presume that this may relate to the genotypic differences in residual activity, and the quantitative assay was able to resolve this. This difference in severity is further evident that in fibroblasts Patient 1 had abnormal complex V on blue native PAGE and abnormalities in complex I assembly, that were not present in the fibroblasts of Patient 2. Yet, both patients had clearly decreased amounts of MT-CO1 in fibroblasts, and borderline low complex IV activity.

There are tissue specific differences. The enzyme deficiency was most pronounced in cardiac muscle tissue, where there was massive proliferation of mitochondria on electron microscopy displacing contractile elements. In skeletal muscle there was also deficient enzyme activity of complexes I and IV in both patients, but to a lesser extent than in heart. In fibroblasts, there was a borderline deficiency of complex IV activity only in both patients. Indeed, the primary clinical presentation also affected heart tissue primarily in our patients and in the previously reported patients.

The cause for the decreased activity appears in the synthesis of the mtDNA encoded proteins. It is remarkable that the activity of complex IV appeared to be somewhat more affected than that of complex I. This was also similarly observed in previously reported patients [4]. In many mitochondrial transcription and translation defects, complex I, which has seven mtDNA-encoded subunits, is affected more pronounced than complex IV which has only three mtDNA-encoded subunits or complex III which has only a single mtDNA-encoded subunit. A greater involvement of complex IV has also been reported for certain other disorders such as *LRPPRC* and *TACO1* [25,26]. The reason for this more pronounced defect in complex IV is not clear. The decrease in the rate of synthesis of the newly formed mtDNA-encoded subunits of complex IV (MT-CO1, MT-CO2, MT-CO3) appeared similarly affected to that of proteins from complex I (MT-ND5, MT-ND2, MT-ND1) and that of complex V (MT-ATP6). A similar decrease in protein synthesis between complex I and complex IV but less than for complexes III and V was previously noted [6]. Thus, it does not appear to be due to a difference in the synthesis rate of the different subunits. A difference in the stability of synthesized proteins could not be excluded.

The decrease in mitochondrial protein synthesis affected respiratory chain function. In Patient 1, oxygen consumption was decreased in fibroblasts, and in Patient 2, the rate of substrate oxidation in muscle tissue was affected. This shows that regardless of tissue, the impact on mitochondrial function was demonstrable. Since the amount of residual activity is related to translational efficiency, to improve the function and perhaps allow infants to recover from the cardiac dysfunction, increasing the amount of ml44 should be considered. Upregulators of the expression of MRPL44 such as mitochondrial biogenesis inducers such as Nrf2 activators, PGC1-α activators or PPAR-δ activators could be explored [27–29].

In conclusion, pathogenic variants in *MRPL44* are a cause of infantile cardiomyopathy. They reduce the amount of ml44 protein which causes a reduction the synthesis of mtDNA-encoded proteins with a resulting combined deficiency with emphasis on complex I and IV impairing oxidative phosphorylation activity. The degree of oxidative phosphorylation dysfunction correlated with the impairment of mitochondrial protein synthesis due to different pathogenic variants. These functional studies allow for improved understanding of the pathogenesis of MRPL44-associated mitochondrial disorder.

Supplementary Material

Refer to Web version on PubMed Central for supplementary material.

Acknowledgments

Financial support for this study was received from Children's Hospital Colorado Foundation, Summits for Samantha and Miracles for Mito (JVH, MWF, KMK). JVH, KMK, and MWF are supported by a grant from the National Institutes of Health, NIH U54NS078059 for the North American Mitochondrial Disease Consortium (NAMDC). NAMDC is part of Rare Diseases Clinical Research Network (RDCRN), an initiative of the Office of Rare Diseases Research (ORDR), NCATS. This consortium is funded through collaboration with NCATS. Contents are the authors' sole responsibility and do not necessarily represent official NIH views. The study was also supported by the Austrian Science Fund (FWF) GENOMIT I 4695-B to JAM. HP was supported by a German Federal Ministry of Education and Research (BMBF, Bonn, Germany) research grant "German Network for Mitochondrial Disorders" (mitoNET, 01GM1906B); by the German BMBF and Horizon2020 through the E-Rare project GENOMIT (01GM1920A) and the ERA PerMed project PerMiM (01KU2016A). Funding sources had no role in the design or execution of the study, in the interpretation of data or the writing of the study.

7. References:

1. Scaglia F, Towbin JA, Craigen WJ, Belmont JW, Smith EO, Neish SR, Ware SM, Hunter JV, Fernbach SD, Vladutiu GD, Wong LJ, Vogel H. Clinical spectrum, morbidity, and mortality in 113 pediatric patients with mitochondrial disease. Pediatrics 2004;114:925–931. [PubMed: 15466086]
2. Towbin JA. Mitochondrial cardiology. In: DiMauro S, Hirano M, Schon EA (Eds) Mitochondrial Medicine, Informa Healthcare, Abingdon UK, 2006 pp. 75–103.
3. Boczonadi V, Ricci G, Horvath R. Mitochondrial DNA transcription and translation: clinical syndromes. Essays Biochem 2018;62(3):321–340. [PubMed: 29980628]
4. Carroll CJ, Isohanni P, Pöyhönen R, Euro L, Richter U, Brilhante V, Götx A, Lahtinen T, Paetau A, Pihko H, Battersby BJ, Tyynismaa H, Suomalainen A. Whole-exome sequencing identifies a mutation in the mitochondrial ribosome protein MRPL44 to underlie mitochondrial infantile cardiomyopathy. J Med Genet 2013;50:151–159. [PubMed: 23315540]
5. Distelmaier F, Haack TB, Catarino CB, Gallenmüller C, Rodenburg RJ, Strom TM, Baertlin F, Meitinger T, Mayatepek E, Prokisch H, Klopstock T. *MRPL44* mutations cause a slowly progressive multisystem disease with childhood-onset hypertrophic cardiomyopathy. Neurogenet 2015;16:319–323.
6. Horga A, Manole A, Mitchell AL, Bugiardini E, Hargreaves IP, Mowafi W, Bettencourt C, Blakely EL, He L, Polke JM, Woodward CE, Dalla Rosa I, Shah S, Pittman AM, Quinlivan R, Reilly MM, Taylor RW, Holt IJ, Hanna MG, Pitceathly RD S, Spinazzola A, Houlden H. Uniparental isodisomy of chromosome 2 causing *MRPL44*-related multisystem mitochondrial disease. Mol Biol Rep 2021; 3 19, Epub available ahead of print
7. Koc EC, Burkhart W, Blackburn K, Moyer MB, Schlatzer DM, Moseley A, Spremulli LL. The large subunit of the mammalian mitochondrial ribosome. Analysis of the complement of ribosomal proteins present. J Biol Chem 2001;276:43958–43969. [PubMed: 11551941]
8. De Silva D, Tu Y-T, Amunts A, Fontanesi F, Barrientos A. Mitochondrial ribosome assembly I health and disease. Cell Cycle 2015;14:2226–2250. [PubMed: 26030272]

9. Yeo JHC, Skinner JPJ, Bird MJ, Formosa LE, Zhang J-G, Kluck RM, Belz GT, Chong MMW. A role for the mitochondrial protein Mprl44 in maintaining OXPHOS capacity. PLoS ONE 10(7):e0134326

10. Greber BJ, Ban N. Structure and function of the mitochondrial ribosome. Annu Rev Biochem 2016;85:103–132. [PubMed: 27023846]

11. Zeng R, Smith E, Barrientos Yeast mitoribosome large subunit assembly proceeds by hierarchical incorporation of protein clusters and modules on the inner membrane. Cell Metab 2018;27:645–656. [PubMed: 29514071]

12. Cheong A, Lingutla R, Mager J. Expression analysis of mammalian mitochondrial ribosomal protein genes. Gene Expr Patterns 2020; 38:119147. [PubMed: 32987154]

13. Kremer LS, Bader DM, Mertes C, Kopajtich R, Pichler G, Iuso A, Haack TB, Graf E, Schwarzmayr T, Terrile C, Koňaříková E, Repp B, Kastenmüller G, Adamski J, Lichtner P, Leonhardt C, Funalot B, Doanti A, Tiranti V, Lombes A, Jardel C, Gläser D, Taylor R Wm Ghezzi D, Mayr JA, Rötig A, Freisinger P, Distelmaier F, Strom TM, Meitinger T, Gagneur J, Prokisch H. Genetic diagnosis of Mendelian disorders via RNA sequencing. Nat Commun. 2017;8(1):1–11. [PubMed: 28232747]

14. Wagner M, Berutti R, Lorenz-Depiereux B, Graf E, Eckstein G, Mayr JA, Meitinger T, Ahting U, Prokish H, Strom TM, Wortmann SB. Mitochondrial DNA mutation analysis from exome sequencing – A more holistic approach in diagnostics of suspected mitochondrial disease. J Inherit Metab Dis 2019;42:909–917. [PubMed: 31059585]

15. Chatfield KC, Coughlin CR 2nd, Friederich MW, Gallagher RC, Hesselberth JR, Lovell MA, Ofman R, Swanson MA, Thomas JA, Wanders RJ, Wartchow EP, Van Hove JLK. Mitochondrial energy failure in HSD10 disease is due to defective mtDNA transcript processing. Mitochondrion 2015;21:1–10. [PubMed: 25575635]

16. Coughlin CR 2nd, Scharer GH, Friederich MW, Yu HC, Geiger EA, Creadon-Swindell G, Collins AE, Vanlander AV, Coster RV, Powell CA, Swanson MA, Minczuk, Van Hove JL, Shaikh TH. Mutations in the mitochondrial cysteinyl-tRNA synthase gene, CARS2, lead to a severe epileptic encephalopathy and complex movement disorder. J Med Genet 2015;52:532–540. [PubMed: 25787132]

17. Van Coster R, Smet J, George E, De Meirleir L, Seneca S, Van Hove J, Sebire G, Verhelst H, De Bleecker J, Van Vlem B, Verloo P, Leroy J. Blue native polyacrylamide gel electrophoresis: a powerful tool in diagnosis of oxidative phosphorylation defects. Pediatr Res 2001;50:658–665. [PubMed: 11641463]

18. Rustin P, Chretien D, Bourgeron T, Gérard B, Rötig, Saudubray JM, Munnich A. Biochemical and molecular investigations in respiratory chain deficiency. Clin Chim Acta 1994;228(1):35–51. [PubMed: 7955428]

19. Mayr JA, Paul J, Pecina P, Kurnik P, Förster H, Fötschl U, Sperl W, Houštěk J. Reduced respiratory control with ADP and changed pattern of respiratory chain enzymes as a result of selective deficiency of the mitochondrial ATP synthase. Pediatr Res 2004;55:988–994. [PubMed: 15155867]

20. Bookelman H, Trijbels JM, Sengers RC, Janssen AJ, Veerkamp JH, Stadhouders AM. Pyruvate oxidation in rat and human skeletal muscle mitochondria. Biochem Med 1978;20:395–403. [PubMed: 752349]

21. Friederich MW, Erdogan AJ, Coughlin CRII, Elos M, Jiang H, O'Rourke C, Lovell MA, Wartchow E, Gowan K, Chatfield KC, Chick WS, Spector E, Van Hove JLK, Riemer J. Mutations in the accessory subunit NDUFB10 result in isolated complex I deficiency and illustrate the critical role of intermembrane space import for complex I holoenzyme assembly. Hum Mol Genet 2017;26:702–716. [PubMed: 28040730]

22. Sasarman F, Shoubridge EA. Radioactive labeling of mitochondrial translation products in cultured cells. Methods Mol Biol 2012;837:207–217. [PubMed: 22215550]

23. Friederich MW, Timal S, Powell CA, Dallabona C, Kurolap A, Palacios-Zambrano S, Bratkovic D, Derks TGJ, Bick D, Bouman K, Chatfield KC, Damouny-Naoum N, Dishop MK, Falik-Zaccai TC, Fares F, Fedida A, Ferrero I, Gallagher RC, Garesse R, Gilberti M, González C, Gowan K, Habib C, Halligan RK, Kalfon L, Knight K, Lefeber D, Mamblona L, Mandel H, Mory A, Ottoson J, Paperna T, Pruijn GJM, Rebelo-Guiomar PFR, Saada A, Sainz B Jr, Salvemini H, Schoots MH,

Smeitink JA, Szukszto MJ, ter Horst HJ, van den Brandt F, van Spronsen FJ, Veltman JA, Wartchow E, Wintjes LT, Zohar Y, Fernández-Moreno MA, Baris HN, Donnini C, Minczuk M, Rodenburg RJ, Van Hove JLK. Mutations in the genes QRSL1, GATB, and GATC encoding the subunits of glutamyl-tRNAGln amidotransferase cause a lethal mitochondrial disorder with cardiomyopathy. Nat Commun 2018;9:4065 [PubMed: 30283131]

24. Gray VE, Hause RJ, Fowler DM. Analysis of large-scale mutagenesis data to assess the impact of single amino acid substitutions. Genetics 2017;207:53–61. [PubMed: 28751422]
25. Oláhová M, Hardy SA, Hall J, Yarham JW, Haack TB, Wilson WC, Alston CL, He L, Aznauryan E, Brown RM, Braon GK, Morris AAM, Mundy H, Broomfield A, Barbosa IA, Simpson MA, Deshpande C, Moeslinger D, Koch J, Stettner GM, Bonnen PE, Prokisch H, Lightowlers RN, McFarland R, Chrzanowska-Lightowlers ZMA, Taylor RW. LRPPRC mutations cause early-onset multisystem mitochondrial disease outside of the French-Canadian population. Brain 2015;138:3503–3519. [PubMed: 26510951]
26. Weraarpachai W, Antonicka H, Sasarman F, Seeger J, Schrank B, Kolesar JE, Lochmüller H, Chevrette M, Kaufman BA, Horvath R, Shoubridge EA. Mutation in TACO1, encoding a translational activator of COX1, results in cytochrome c oxidase deficiency and late-onset Leigh syndrome. Nat Genet 2009;41(7):833–837. [PubMed: 19503089]
27. Pitcedathly RDS, Keshavan N, Rahman J, Rahman S. Moving towards clinical trials for mitochondrial diseases. J Inherit Metab Dis 2021;44(1):22–41. [PubMed: 32618366]
28. Dinkova-Kostova AT< Abramov AY. The emerging role of Nrf2 in mitochondrial function. Free Radical biol Med 2015;88:179–188 [PubMed: 25975984]
29. Steele H, Gomez-Duran A, Pyle A, Hopton S, Newman J, Stefanetti RJ,Charman SJ, Parikh JD, He L, Viscomi C, Jakovljevic DG, Hollingsworth KG, Robinson AJ, Taylor RW, Tottolo L, Horvath R, Chinnery PF. Metabolic effects of bezafibrate in mitochondrial disease. EMBO Mol Med 2020;12(3):e11589. [PubMed: 32107855]
30. Vasilescu C, Ojala TH, Brilhante V, Ojanen S, Hinterding HM, Palin E, Alastalo T-P, Koskenvuo J, Hiipala A, Jokinen E, Jahnukainen T, Lohi J, Pihkala J, Tyni TA, Carroll CJ, Suomalainen A. Genetic basis of severe childhood-onset cardiomyopathies. J Am Coll Cardiol 2018;72(19):2324–2338. [PubMed: 30384889]

Highlights:

1. Patients with MRPL44-disorder clinically present in infancy with cardiomyopathy, and survivors develop encephalomyopathy in childhood to early adulthood
2. MRPL44-disorder causes a defect of mitochondrial translation impairing the synthesis of all mitochondrial DNA encoded subunits and thus causing a combined oxidative phosphorylation deficiency
3. The degree of biochemical impairment may be related to the residual activity of the pathogenic variant.

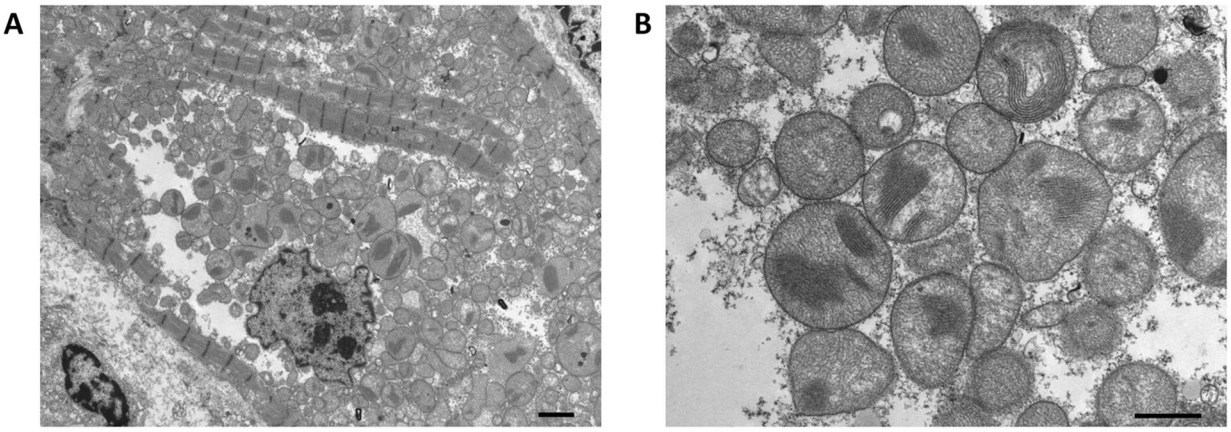

Figure 1: Electron microscopy of the heart

Electron microscopic examination shows areas of contractile element loss within the cardiomyocytes (A) and a diffuse profusion of enlarged, atypically shaped mitochondria with aberrant cristae (B). The scale bar in A represents 2 μm and in B represents 1 μm.

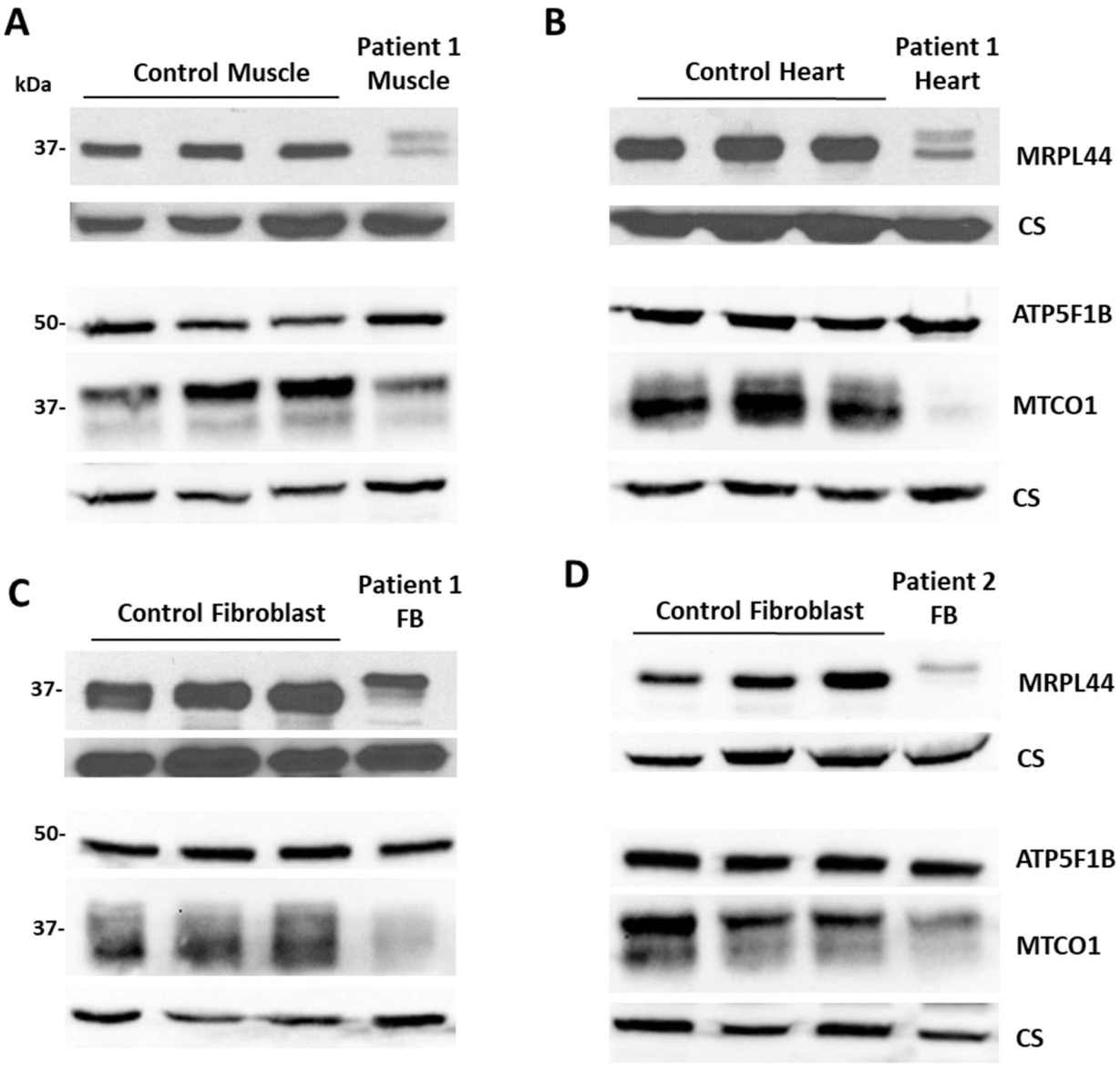

Figure 2: Mitochondrial protein amounts of ml44, MTCO1, and ATP5FB1 by western blot analysis

Protein amounts for ml44, MTCOI and ATP5FB1 are shown after separation on an SDS-PAGE gel, followed by western blotting in Patient 1 heart muscle (A) skeletal muscle (B) and fibroblasts (C) and in Patient 2 fibroblasts (D). The ml44 protein is reduced in the heart muscle, skeletal muscle and fibroblasts in Patient 1 and in fibroblasts from Patient 2. In heart and skeletal muscle, the ml44 protein appears as a double band, one similar to that of controls, and an added band of slightly higher molecular weight. In fibroblasts, only the band with a slightly higher MW is visible. The MTCOI protein is reduced in the heart muscle, skeletal muscle and fibroblasts in Patient 1 and in fibroblasts from Patient 2 but the amount of the ATP5FB1 protein in both patients is not reduced compared to the control samples. Citrate synthase is used as a loading control.

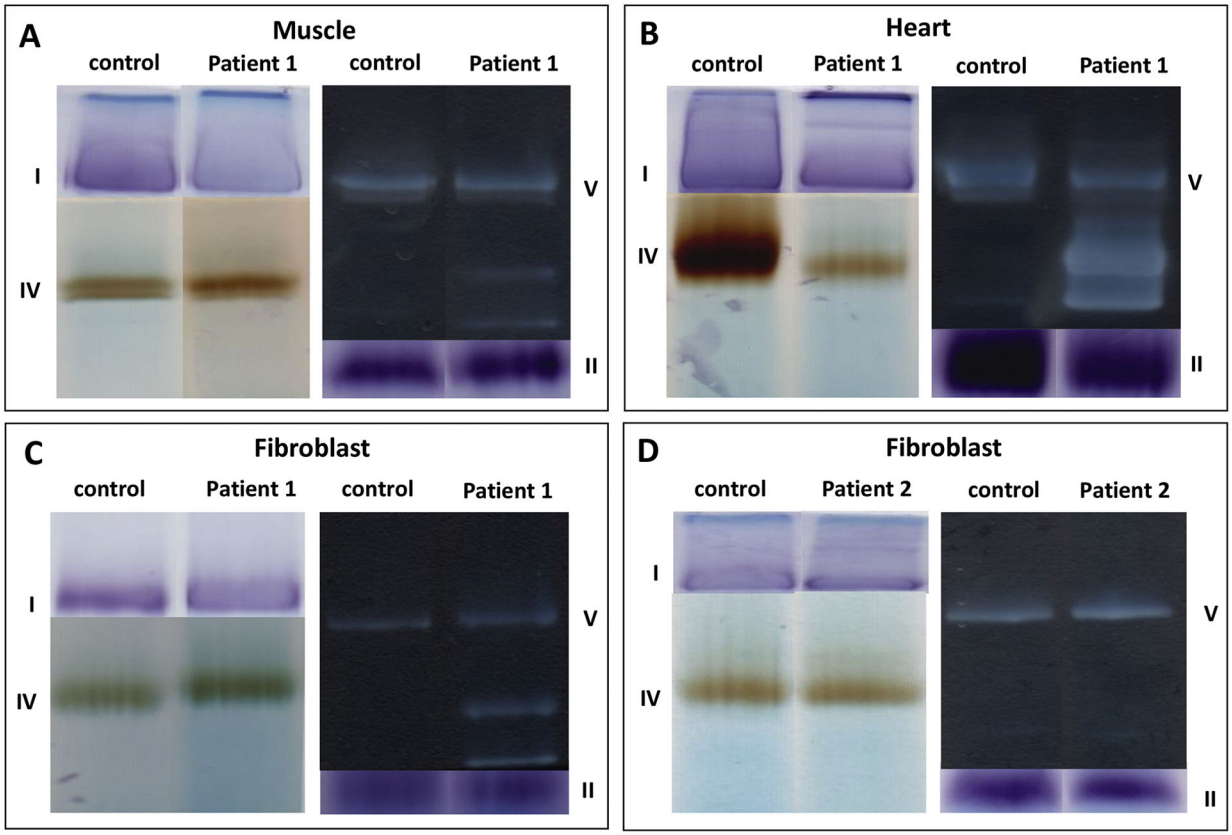

Figure 3: Mitochondrial enzyme complexes evaluated by blue native polyacrylamide gel separation with in-gel activity staining

The activity of complexes I, II, IV, and V is shown by in-gel activity staining following separation on a blue native polyacrylamide gel electrophoresis in Patient 1 (A) heart muscle (B) skeletal muscle and (C) fibroblasts, and in (D) Patient 2 fibroblasts. Complex IV staining is reduced in heart muscle. Complex V staining reveals the presence of two additional bands representing incompletely assembled F_1 subunits, not present in controls, as is typically observed when the mitochondrial DNA encoded subunits of complex V are insufficiently present. In the fibroblasts of Patient 2, no abnormalities were observed.

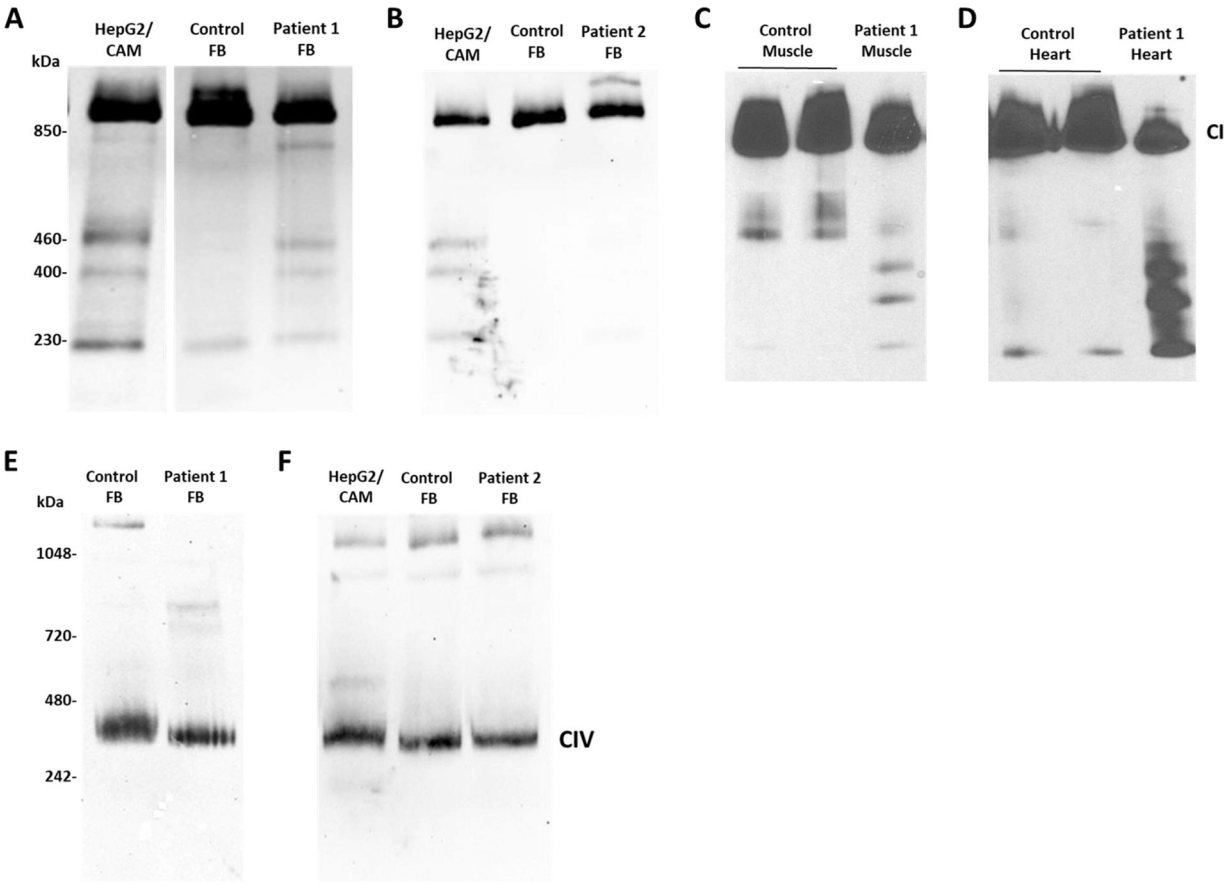

Figure 4: Examination of the assembly of complexes I and IV using non-denaturing polyacrylamide gel followed by western blot

(A–D) The assembly of complex I is shown by separation on a non-denaturing polyacrylamide gel followed by western blotting and detection with an antibody against NDUFS2 in Patient 1 and Patient 2 in comparison to controls and HepG2 cells treated with chloramphenicol. (A) Control fibroblasts show in addition to the fully assembled holocomplex, a faint band at 230 kDa, whereas as Patient 1 shows additional bands at 400, 460, and 850 kDa. (B) Assembly of complex I in Patient 2 in fibroblasts is normal. (C) In skeletal muscle from Patient 1, control samples show in addition to the holocomplex typical additional bands at 400 and 460 kDa, whereas the patient's sample also showed abnormal bands at 100 and 230 kDa. (D) In heart muscle, control samples show in addition to the holocomplex also a faint band at 100 kDa, and in the patient sample additional bands at 230, 400 and 460 kDa were present. (E,F) The assembly of complex IV is shown by separation on a non-denaturing polyacrylamide gel followed by western blotting and detection with an antibody against COXIV in Patient1 and Patient 2. No abnormal intermediates are seen in Patient 1 (E) and Patient 2 (F).

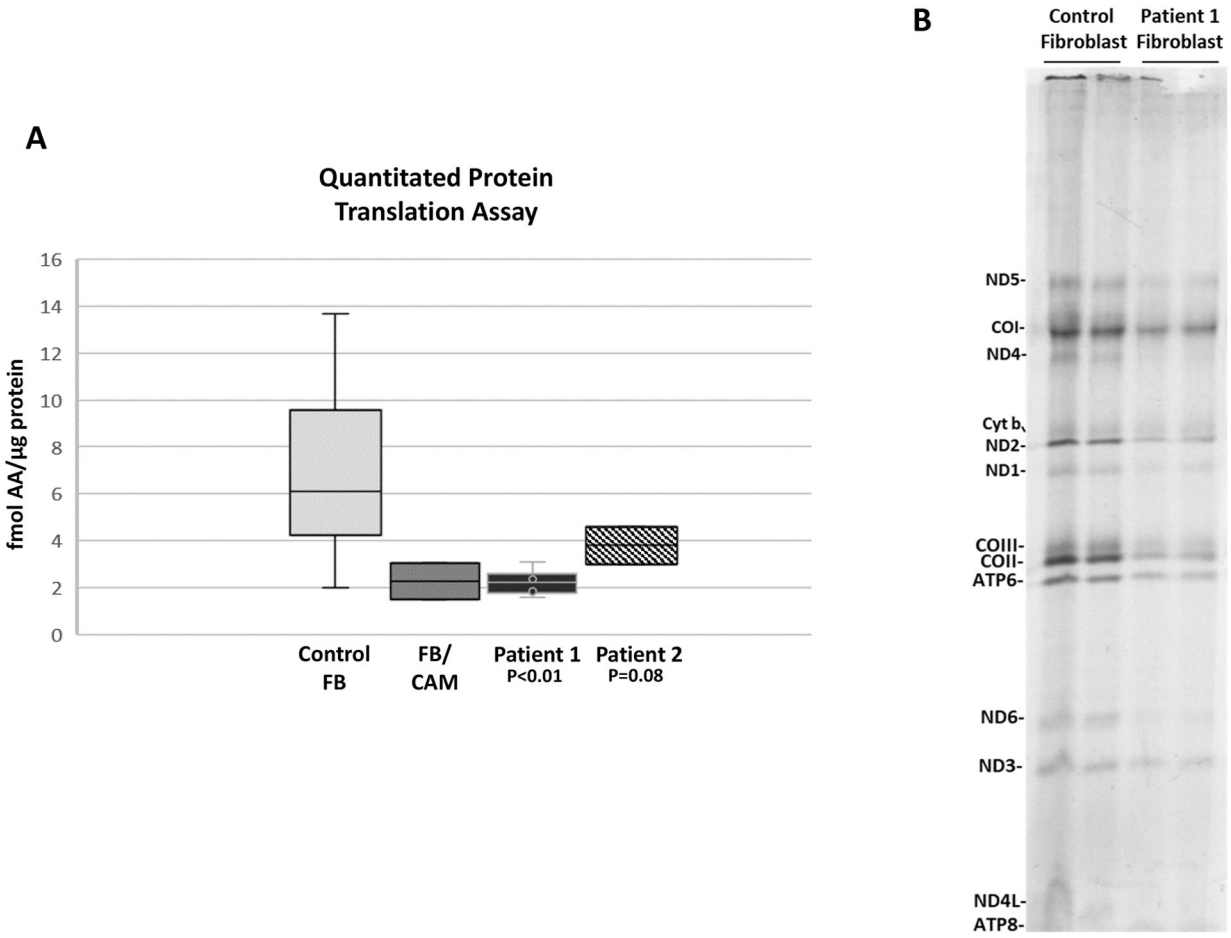

Figure 5: Mitochondrial protein synthesis in fibroblasts of Patient 1 and Patient 2

Mitochondrial DNA encoded proteins are labeled with ^{35}S-methionine and ^{35}S-cysteine in fibroblasts. (A) In a quantitative assay the amount of radioactive incorporation into proteins is reduced in fibroblasts of Patient 1 to a similar degree as of inhibition of mitochondrial protein synthesis by chloramphenicol, but to a lesser extent in Patient 2. (B) Labeled proteins are separated on an SDS-PAGE gel showing two controls in comparison with two samples from Patient 1. The samples show a reduction in each of the protein bands.

Mol Genet Metab. Author manuscript; available in PMC 2022 August 01.

Table 1:

Mitochondrial respiratory chain enzyme activities

PATIENT 1	**Activity (controls) nmol.min^{-1}.mg protein**	**SD**	**Ratio enzyme/CS**	**SD**	**Ratio enzyme/complex II**	**SD**
SKELETAL MUSCLE						
Complex I	35.1 (23.6 – 74.8)	−0.5	**85** (98–271)	−1.6	**182** (285–767)	**−2.6**
Complex II	**192.4** (49.0 – 133.4)	**+2.5**	468 (251–573)	+1.3	NA	NA
Complex III	45.9 (5.7 – 31.4)	+1.8	112 (19 – 172)	+1.3	238 (45 – 369)	+0.9
Complex II–III	75.4 (34.2 – 107.6)	+0.7	183 (172 – 472)	−0.6	**392** (549 – 1226)	−1.7
Complex IV	1.6 (1.1 – 3.8)	−0.9	**4** (4 – 23)	−1.0	**9** (11 – 68)	−1.1
Citrate synthase	**411.5** (159.8 – 353.3)	+1.9	NA	NA	NA	NA
HEART						
Complex I	**44.9** (146.9 – 366.9)	**−5.3**	**55** (144 – 376)	**−5.2**	**158** (506 – 1064)	**−5.9**
Complex II	284.3 (176.4 – 412.5)	−0.1	351 (235 – 356)	+1.2	NA	NA
Complex III	54.0 (16.5 – 260.4)	−0.2	67 (12 – 210)	+0.0	190 (45 – 680)	−0.1
Complex II–III	**120.1** (176.2 – 546.0)	**−2.1**	**148** (189 – 433)	**−2.2**	**422** (680 – 1468)	**−2.6**
Complex IV	**0.9** (12.0 – 32.0)	**−10.1**	**1** (11 – 32)	**−10.2**	**3** (36 – 100)	**−10.5**
Citrate synthase	810.8 (497.4 – 1473.3)	−0.7	NA	NA	NA	NA
FIBROBLASTS						
Complex I	55.5 (49.3–131.1)	−1.4	172 (145–396)	−1.1	197 (237–754)	−1.8
Complex II	281.5 (130.9–364.4)	+0.7	870 (297–863)	+1.3	NA	NA
Complex III	12.0 (8–29.2)	−0.4	37 (19–65)	−0.2	47 (36–114)	−0.7
Complex II–III	126.9 (61.8–158.8)	+0.6	392 (131–376)	+1.3	451 (263–1100)	−0.1
Complex IV	**2.0 (2.2–7.1)**	**−2.0**	**6 (6–23)**	**−2.0**	**7 (12–35)**	**−2.2**
Citrate synthase	323.4 (253.5–554.1)	−0.7	NA	NA	NA	NA
PATIENT 2	Activity (controls)		Ratio enzyme/CS			
SKELETAL MUSCLE						
Complex I	**16** (28–76)		**0.13** (0.14–0.35)			
Complex I–III	63 (49–218)		0.52 (0.24–0.81)			
Complex II	42 (33–102)		0.35 (0.18–0.41)			

PATIENT 1	Activity (controls) nmol.min^{-1}.mg protein	SD	Ratio enzyme/CS	SD	Ratio enzyme/complex II	SD
Complex III	**125** (304–896)		**1.02** (1.45–3.76)			
Complex II–III	80 (65–180)		0.65 (0.3–0.67)			
Complex IV	**62** (181–593)		**0.51** (0.91–2.24)			
Complex V	**77** (86–257)		0.63 (0.42–1.26)			
PDH	**4.2** (5.3–19.8)		0.034 (0.026–0.08)			
Citrate synthase	**122** (150–338)		NA			
FIBROBLASTS						
Complex I	89.7 (49.3–131.1)	+0.2	346 (145–396)	+1.4	387 (237–754)	+0.0
Complex II	231.7 (130.9–364.4)	+0.1	894 (297–863)	+1.4	NA	
Complex III	24.4 (8–29.2)	+1.3	94 (19–65)	+2.0	105 (36–114)	+1.4
Complex II–III	106.4 (61.8–158.8)	+0.1	410 (131–376)	+1.4	459 (263–1100)	−0.2
Complex IV	3.9 (2.2–7.1)	−0.3	15 (6–23)	+0.0	17 (12–35)	−0.3
Citrate synthase	259.1 (253.5–554.1)	−1.4	NA	NA	NA	
FIBROBLAST Mitochondrial isolate						
Complex I	21 / 15 (15–53)		0.08 / 0.05 (0.05–0.09)			
Complex I–III	**98 / 50** (102–343)		0.38 / 0.16 (0.24–0.58)			
Complex II	129 / 120 (103–285)		0.50 / 0.38 (0.37–0.48)			
Complex III	1198 / 1174 (283–1174)		4.68 / 3.74 (1.17–1.99)			
Complex II–III	208 / 236 (167–314)		0.81 / 0.75 (0.39–0.72)			
Complex IV	**339 / 306** (392–939)		1.32 / **0.98** (1.10–1.68)			
Complex V	198 / 115 (36–167)		0.78 / 0.37 (0.15–0.39)			
PDH	6.9 / 8.8 (6.0–19.7)		0.027 / 0.028 (0.014–0.050)			
Citrate synthase	256 / 314 (242–590)		NA			

The activities of each respiratory chain complex and of combined complex activities I-III or II-III are shown expressed as nmol.min^{-1}.mg protein, and as the ratio over the activity of citrate synthase and as a ratio over the activity of complex II. The values are also expressed for Case 1 as standard deviations (Z-score) of the log transformed values of controls, which are normally distributed. The activity of complex V is reported in the direction of hydrolytic ATPase activity. The activity of the patient is shown with the range of controls in brackets.

Table 2:

High resolution respirometry in fibroblasts

Patient 1: oxygen consumption in pmol oxygen.sec^{-1}.10^6 cells				
Parameter	**Patient (n=6)**	**Control (n=41)**		
	Mean±SD	**Mean±SD**	**5th – 95th percentile**	**t-test p value**
Pyruvate	13.31±4.62	15.5±13.1	5.9–43.6	**0.038**
Pyruvate+ADP	14.55±5.88	30.5±14.0	14.2–63.1	**0.009**
Acceptor control ratio	1.93±0.55	2.96±1.45	1.22–4.42	0.09
Pyruvate+Glutamate+ADP	14.5±5.86	31.55±14.57	7.41–58.61	**0.007**
Pyruvate+Glutamate+Succinate+ADP	30.26±12.58	42.9±14.6	23.0–80.3	**0.05**
Uncoupled P+G+S+CCCP	**34.55**±12.84	83.0±23.7	45.9–139.5	**<0.001**
Uncoupling increase	**4.29**±6.54	40.1±16.5	9.6–65.6	**<0.001**
Coupling control ratio	**0.89**±0.21	53.0±14.6%	34%–83%	**<0.001**
Complex I	**17.79**±7.60	61.6±22.2	31.6–123.2	<0.001
Complex IV	**24.67**±14.28	70.6±28.3	30.8–108.2	**<0.001**

The oxygen consumption in pmol oxygen.sec^{-1}.10^6 cells is shown for a replicate of 6 fibroblast cell preparations from Patient 1 and compared to that of 41 control fibroblast cell lines, average of duplicates. Abbreviations: P = pyruvate, G = glutamate, S= succinate, ADP = adenosine diphosphate, CCCP = Carbonyl cyanide 3-chlorophenylhydrazone. The complex I rate is the uncoupled rate minus the rate with the addition of rotenone, and the complex IV is measured as the rate with tetramethyl-p-phenylenediamine (TMPD) + ascorbate minus the rate after addition with azide. The acceptor control ratio is the ratio of the ADP stimulated pyruvate rate over the non-ADP rate, and the coupling control ratio is the percent of ADP stimulated maximal rate from the uncoupled rate.